

From autoinhibition to inhibition in trans: the Raf-1 regulatory domain inhibits Rok- α kinase activity

Théodora Niault,¹ Izabela Sobczak,¹ Katrin Meissl,¹ Gregory Weitsman,^{2,3,4} Daniela Piazzolla,¹ Gabriele Maurer,¹ Florian Kern,¹ Karin Ehrenreiter,¹ Matthias Hamerl,¹ Ismail Moarefi,⁵ Thomas Leung,⁶ Oliviero Carugo,^{1,7} Tony Ng,^{2,3,4} and Manuela Baccarini¹

¹Max F. Perutz Laboratories, Center for Molecular Biology, University of Vienna, 1030 Vienna, Austria

²Richard Dimbleby Department of Cancer Research, ³Randall Division of Cell and Molecular Biophysics, and ⁴Division of Cancer Studies, King's College London, WC2R 2LS London, England, UK

⁵CRELUX GmbH, 82152 Martinsried, Germany

⁶Institute of Molecular and Cell Biology, Singapore 138673

⁷Department of General Chemistry, University of Pavia, 27100 Pavia, Italy

The activity of Raf-1 and Rok- α kinases is regulated by intramolecular binding of the regulatory region to the kinase domain. Autoinhibition is relieved upon binding to the small guanosine triphosphatases Ras and Rho. Downstream of Ras, Raf-1 promotes migration and tumorigenesis by antagonizing Rok- α , but the underlying mechanism is unknown. In this study, we show that Rok- α inhibition by Raf-1 relies on an intermolecular interaction between the Rok- α kinase domain and the cysteine-rich

Raf-1 regulatory domain (Raf-1reg), which is similar to Rok- α 's own autoinhibitory region. Thus, Raf-1 mediates Rok- α inhibition in trans, which is a new concept in kinase regulation. This mechanism is physiologically relevant because Raf-1reg is sufficient to rescue all Rok- α -dependent defects of Raf-1-deficient cells. Downstream of Ras and Rho, the Raf-1–Rok- α interaction represents a novel paradigm of pathway cross talk that contributes to tumorigenesis and cell motility.

Introduction

The GTPases Rho, Rac, and Cdc42 control fundamental processes including cell shape, polarity, and migration but also gene expression and cell cycle progression. Thus, Rho GTPases and their effectors are promising therapeutic targets for several diseases, including cancer (Heasman and Ridley, 2008; Olson, 2008).

The Rho effectors Rok- α and - β (Riento and Ridley, 2003; Zhao and Manser, 2005) are serine/threonine kinases with a modular structure comprising an N-terminal catalytic domain, a coiled-coil region containing the Ras/Rho-binding

domain (RBD), and a C-terminal regulatory region with an unusual pleckstrin homology (PH) domain interrupted by a cysteine-rich domain (CRD; Riento and Ridley, 2003). Roks are regulated by autoinhibition; their C-terminal regulatory region, particularly the PH/CRD domain, binds to the kinase domain and inhibits its activity (Amano et al., 1999; Chen et al., 2002). Interaction of two RhoA molecules with the RBD domains arranged in a parallel coiled-coil dimer relieves autoinhibition (Amano et al., 1999; Shimizu et al., 2003; Dvorsky et al., 2004) and leads to kinase domain dimerization, trans-autophosphorylation, and activation (Riento and Ridley, 2003; Zhao and Manser, 2005).

Raf-1, a serine/threonine kinase member of the Ras/extracellular signal-regulated kinase (ERK) signaling pathway, interacts with Rok- α (Ehrenreiter et al., 2005; Piazzolla et al., 2005). In Raf-1 knockout (KO) cells, hyperactive Rok- α causes cytoskeletal changes, leading to inhibition of cell migration

© 2009 Niault et al. This article is distributed under the terms of an Attribution-Noncommercial-Share Alike-No Mirror Sites license for the first six months after the publication date (see <http://www.jcb.org/misc/terms.shtml>). After six months it is available under a Creative Commons License (Attribution-Noncommercial-Share Alike 3.0 Unported license, as described at <http://creativecommons.org/licenses/by-nc-sa/3.0/>).

I. Sobczak and K. Meissl contributed equally to this paper.

Correspondence to Manuela Baccarini: manuela.baccarini@univie.ac.at

K. Meissl's present address is Nederlands Kanker Instituut, 1066 CX Amsterdam, Netherlands.

D. Piazzolla's present address is Centro Nacional de Investigaciones Oncológicas, E-28029 Madrid, Spain.

Abbreviations used in this paper: CRD, cysteine-rich domain; ERK, extracellular signal-regulated kinase; FLIM, fluorescent lifetime imaging microscopy; FRET, fluorescence resonance energy transfer; KO, knockout; MEF, mouse embryonic fibroblast; MEK, MAPK/ERK kinase; mRFP, monomeric RFP; PH, pleckstrin homology; Raf-1reg, Raf-1 regulatory domain; Rok- α reg, Rok- α regulatory domain; RBD, Ras/Rho-binding domain; WT, wild type.

(Ehrenreiter et al., 2005) and hypersensitivity to Fas-induced apoptosis (Piazzolla et al., 2005). Intriguingly, Raf-1-mediated inhibition of Rok- α is also essential for Ras-induced tumorigenesis in vivo (Ehrenreiter et al., 2009).

Like Rok- α , Raf-1 is part of a family of kinases recruited to the cell membrane and activated by a small GTPase, in this case, Ras. Raf kinases share a structure featuring three conserved regions (CRs): (1) CR1, with the RBD and the CRD, (2) CR2, rich in S/T residues, and (3) CR3, encompassing the kinase domain. Like Roks, Rafs are regulated by autoinhibition; their N-terminal regulatory domain, particularly the CRD, binds to the kinase domain, suppressing its catalytic activity (Cutler et al., 1998). Raf activation requires Ras binding, membrane recruitment, and phosphorylation of S/T sites in the activation loop of the CR3 region (Wellbrock et al., 2004).

All Raf kinases can activate the MAPK/ERK kinase (MEK)–ERK module, yet the main in vivo roles of Raf-1 in migration, survival, and Ras-induced tumorigenesis are MEK–ERK independent and rely on Raf-1's ability to interact with and inhibit other kinases such as Rok- α (Ehrenreiter et al., 2005; Piazzolla et al., 2005; Ehrenreiter et al., 2009), MST2 (O'Neill et al., 2004), and ASK-1 (Yamaguchi et al., 2004). Until now, the mechanisms underlying this inhibition were unknown.

Negative regulation of the activity of a kinase by other kinases can occur in the context of a negative feedback loop, as does the inhibition of MEK1 by ERK (Eblen et al., 2004; Catalanotti et al., 2009), or in the context of pathway cross talk, as exemplified by the down-regulation of Raf-1 by Akt or PKA (Wellbrock et al., 2004). In these and other cases, negative regulation is achieved by direct phosphorylation of one kinase by the other. In this study, we report a novel form of kinase regulation and pathway cross talk mediated by protein–protein interaction instead of phosphorylation. Upon growth factor stimulation, GTPase binding to Raf-1 and Rok- α relieves autoinhibition, engendering a change from a closed, inactive state to an open, active conformation essential for Raf-1–Rok- α interaction. In the open state, the Raf-1 regulatory domain (Raf-1reg) binds to the kinase domain of Rok- α and inhibits its enzymatic activity directly. This kinase-independent inhibition in trans represents a new paradigm in pathway cross talk and regulation of kinase activity.

Results and discussion

Activation increases Raf-1–Rok- α interaction

In mouse embryonic fibroblasts (MEFs), Raf-1 binds to Rok- α , limiting its activation and cell membrane localization (Ehrenreiter et al., 2005). Raf-1 could conceivably prevent binding of Rok- α to RhoA by competing for or masking the Rho-binding site. Alternatively, Raf-1 could interact with the negative regulatory PH/CRD domain or the kinase domain of Rok- α and stabilize intramolecular autoinhibition. To test these possibilities, we examined the interaction of full-length (FL) Raf-1 with a series of Rok- α deletion mutants (Fig. 1 A). A mutant lacking the PH/CRD domain (Δ PH/CRD) and a truncated protein containing the kinase domain (Rok- α -K) bound to Raf-1 more efficiently than

FL Rok- α (Fig. 1, B and C; and Fig. S1 A). In contrast, Raf-1 hardly interacted with the Rok- α regulatory domain (Rok- α reg; Fig. 1 B). Next, we used multiphoton fluorescence resonance energy transfer (FRET)/fluorescent lifetime imaging microscopy (FLIM) to directly monitor protein–protein interactions in cells. The fraction of FL Raf-1 bound to FL Rok- α in asynchronously growing cells was under the detection limit. However, robust interaction was detected upon coexpression of active RhoA with the FL proteins or using Rok- α -K as an acceptor (Fig. 1, D and E). FRET efficiency was much higher in cell protrusions (28%; Fig. 1 D, inset), suggesting protein accumulation and increased interaction in these locations. In line with the coimmunoprecipitation experiments, these results show that Raf-1 preferentially binds to the kinase domain of Rok- α . They rule out the possibility that Raf-1 inhibits Rok- α activation by competing with RhoA and suggest instead that RhoA favors intermolecular interaction between Rok- α and Raf-1 by disrupting the intramolecular interaction between the kinase and Rok- α reg.

Ras binding similarly disrupts the interaction between the regulatory and kinase domains of Raf-1, rendering both more accessible for intermolecular interactions (Terai and Matsuda, 2005). Indeed, EGF stimulation increased complex formation between endogenous (Fig. 2 A) or ectopically expressed proteins, as shown by both FRET/FLIM and coimmunoprecipitation experiments (Fig. 2, B and C; and Fig. S1 B). Constitutively active Ras or activation of endogenous Ras by a membrane-tethered form of the Ras guanine nucleotide exchange factor SOS (Sibilia et al., 2000) also stimulated Raf-1–Rok- α interaction (Fig. 2 D). Conversely, mutating the Raf-1 RBD (R89L) or CRD (CC165/168SS; CC/SS) significantly reduced complex formation (Fig. 2, E–G). Thus, activation by Ras is both necessary and sufficient to promote Raf-1–Rok- α interaction.

Ras binding induces a conformational change in Raf-1 and recruits it to the membrane to be phosphorylated by activating kinases (Bondeva et al., 2002). Tethering Raf-1 to the membrane by fusing it to the Ki-Ras membrane-targeting signal (Raf-1 CAAX) activates the MEK–ERK pathway (Leevers et al., 1994), but it abolished binding to Rok- α (Fig. 2 E). Thus, the change from a closed to an open conformation mediated by Ras binding is essential both for MEK–ERK activation and Raf-1–Rok- α interaction, but these two functions of Raf-1 take place in distinct subcellular compartments. Indeed, single fluorophore video tracking of Raf proteins has shown that Raf-1 binds to Ras-GTP and activates MEK–ERK in the context of membrane nanoclusters but redistributes to the cytosol when these structures dissolve (Tian et al., 2007). It is tempting to speculate that the activated Raf-1 molecules leaving the membrane may be those that bind Rok- α in vivo.

Raf-1reg binds to Rok- α and inhibits its kinase activity

The R89L and CC/SS mutations may prevent or weaken Ras binding, thus precluding the conformational change that makes Raf-1reg accessible for Rok- α ; alternatively, they may be more directly involved in the interaction with Rok- α . To distinguish between these possibilities, we introduced the R89L and CC/SS mutations in Raf-1reg, which lacks the Raf-1 kinase domain.

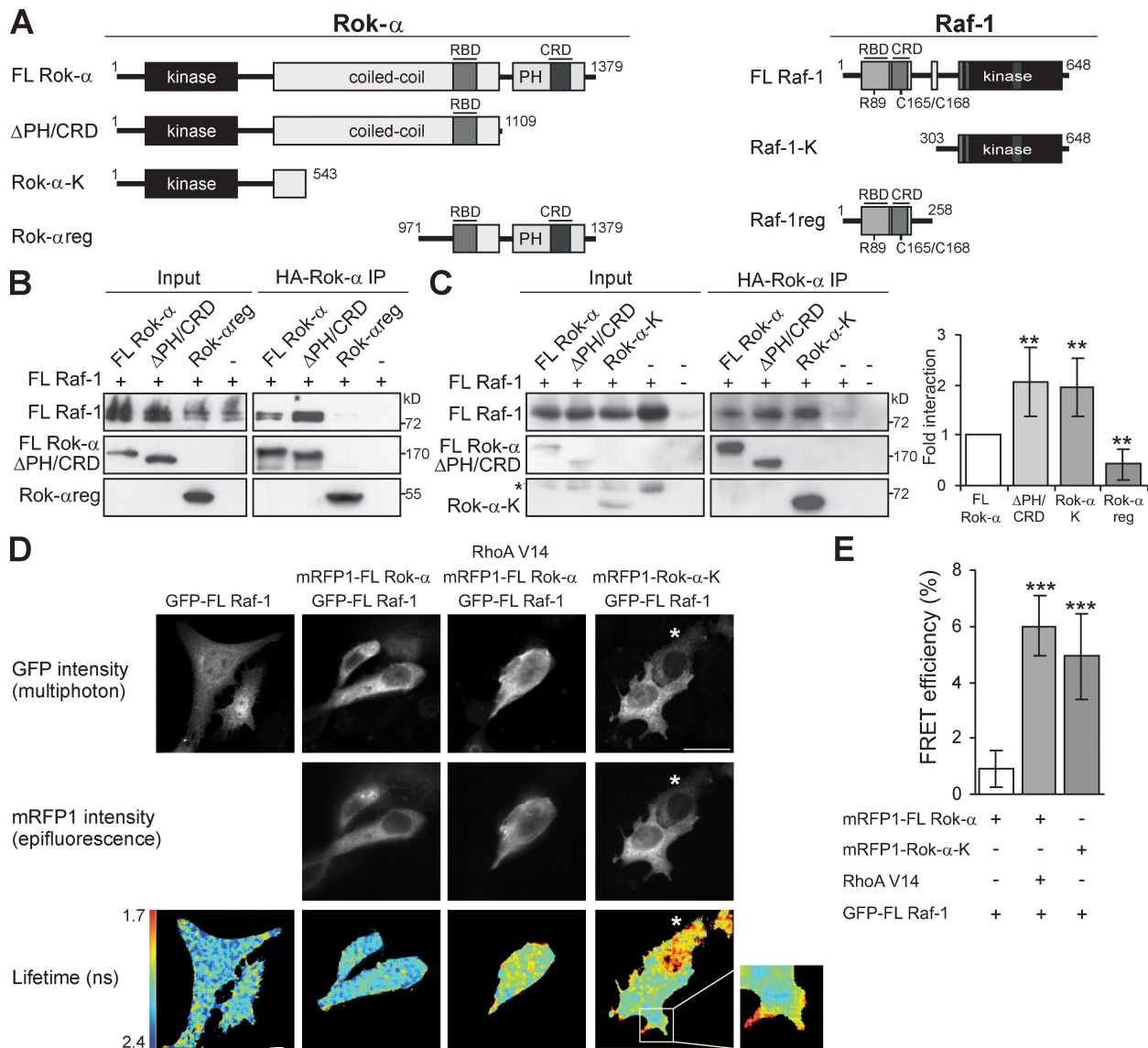


Figure 1. Raf-1 interacts with the Rok- α kinase domain. (A) Rok- α and Raf-1 proteins used in this study are shown. The phosphorylation and Ras-binding site mutants are indicated. (B and C) HA-tagged Rok- α was immunoprecipitated from COS-1 cells cotransfected with Rok- α and FL Raf-1. Input (1.5%) and the immunoprecipitates (IP) were immunoblotted with Raf-1, HA (B), or Rok- α (C) antibodies. *, unspecified band. The amount of Raf-1 coprecipitating with the Rok- α mutant proteins is plotted as fold of FL Raf-1–Rok- α interaction (set as 1; mean \pm SD of four experiments). (D) Fluorescence lifetime (τ), GFP intensity, and mRFP1 intensity in MCF-7 cells transfected with the indicated constructs. RhoAV14 expression was verified by staining with Flag antibody. The cell marked with the asterisks was excluded from the cumulative FRET efficiency analysis in E because of insufficient photon counts (see Material and methods). Inset shows a magnified view of the boxed region. (E) Percentage of FRET efficiency (mean \pm SD of three experiments) is shown. **, $P < 0.01$; ***, $P < 0.005$. Bars, 20 μ m.

In contrast to FL Raf-1 R89L, Raf-1reg R89L retained the ability to coimmunoprecipitate with Rok- α (Fig. 3 A). Thus, binding of Ras-GTP to FL Raf-1 is required solely to disrupt the interaction between the regulatory and kinase domains of Raf-1. Interfering with Ras binding did not increase complex formation with Rok- α , indicating that Ras and Rok- α do not compete for Raf-1.

In contrast, Raf-1reg CC/SS, which binds to Ras but not to the Raf-1 kinase domain (Cutler et al., 1998), failed to associate with Rok- α , implying that the CRD plays a critical role in Raf-1–Rok- α complex formation (Fig. 3 B).

Raf-1 CRD might restrain the activity of Rok- α by binding directly to its kinase domain. Indeed, recombinant GST–

Raf-1reg interacted with Rok- α -K in vitro, pulling down \sim 25% of the Rok- α -K input, whereas GST–Raf-1reg CC/SS was much less efficient (Fig. 3 C). GST–Raf-1reg, but not a CC/SS mutant, reduced Rok- α -K activity in an in vitro kinase assay (Fig. S2). Moreover, Raf-1reg inhibited recombinant Rok- α -K in a dose-dependent manner (\geq 70% inhibition at approximately equimolar concentrations of Raf-1reg and MLC2; Fig. 3 D). The calculated half-maximal inhibitory concentration of 2.65 μ M is fairly high, but this does not prejudice the physiological relevance of the interaction per se, as exemplified by the even lower affinity (20 μ M) of the Raf CRD for Ras-GTP (Williams et al., 2000). Besides, it is unclear how a half-maximal inhibitory concentration calculated in vitro using recombinant proteins relates

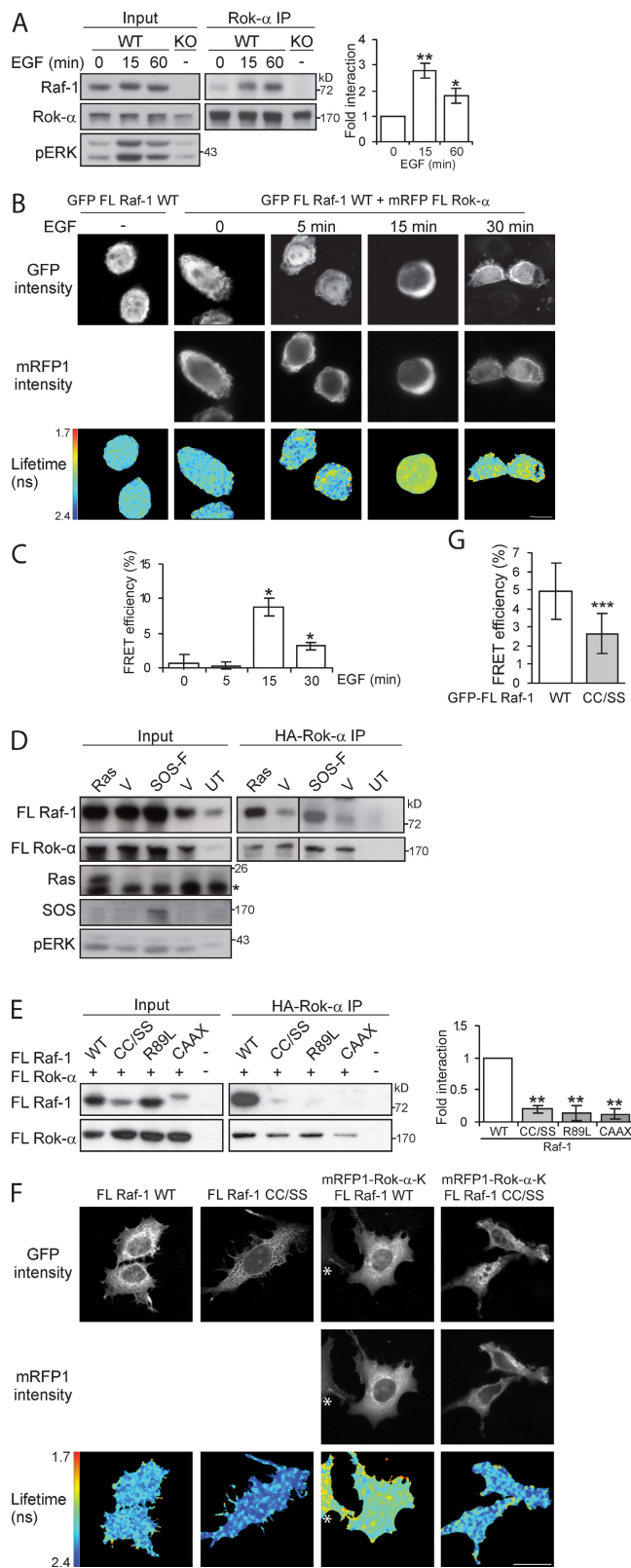


Figure 2. Activated Raf-1 preferentially interacts with Rok- α . (A–C) EGF increases the Rok- α –Raf-1 interaction. (A) MEFs were stimulated with 10 ng/ml EGF, and endogenous Rok- α was immunoprecipitated at the indicated time points. (B and C) Fluorescence lifetime (τ), GFP intensity, and RFP intensity in MDA-MB-468 transfected with GFP-FL Raf-1 and mRFP-FL Rok- α upon stimulation with 100 ng/ml EGF. (C) Percentage of FRET efficiency is shown. Error bars indicate SEM ($n > 3$). (D) Activated Ras promotes Rok- α –Raf-1 interaction. COS-1 cells were transfected with HA-tagged FL Rok- α and indicated FL Raf-1 mutants. HA immunoprecipitates were analyzed and quantified as described in Fig. 1. (E) COS-1 cells were transfected with HA-tagged FL Rok- α and the indicated FL Raf-1 mutants. HA immunoprecipitates were analyzed and quantified as described in Fig. 1. (F) Fluorescence lifetime, GFP intensity, and mRFP1 intensity in MCF-7 cells transfected with GFP-FL Raf-1 WT or CC/SS mutant (donor) and mRFP1-Rok- α -K (acceptor). The cell marked with the asterisk was excluded from the cumulative FRET efficiency analysis in G as a result of insufficient photon counts (see Materials and methods). (G) Percentage of FRET efficiency is shown. (A, E, and G) Error bars indicate SD of three experiments. *, $P < 0.05$; **, $P < 0.01$; ***, $P < 0.005$. Bars: (B) 20 μ m; (F) 30 μ m.

to the binding affinity of the two FL, posttranslationally modified proteins in vivo. Indeed, when expressed at near-endogenous levels in KO MEFs, Raf-1reg wild type (WT), and much less so CC/SS, associated with Rok- α and decreased its kinase activity to levels similar to those observed in WT MEFs (Fig. 3 E).

Concentration of the partners in relevant subcellular compartments will also drive protein–protein interaction in vivo. FL Raf-1 and Rok- α accumulate in membrane protrusions (Fig. 1 D), and both Raf-1 (Ehrenreiter et al., 2005) and Raf-1reg colocalize with Rok- α on filamentous structures (Fig. 4 A) corresponding to the vimentin cytoskeleton. Vimentin is a direct substrate of Rok- α , which by phosphorylating it contributes to its depolymerization (Sin et al., 1998). Vimentin collapses in juxtanuclear aggregates in Raf-1-deficient cells, a phenotype rescued by Raf-1reg (Fig. 4 B). Thus, Raf-1reg is sufficient to mediate the correct localization of Rok- α to the vimentin cytoskeleton and to inhibit Rok- α activity, preventing the collapse of these intermediate filaments. In addition to the vimentin defects, Raf-1 KO cells are contracted and characterized by cortical actin bundles. They contain higher amounts of phosphorylated ezrin than WT cells, and their migration is impaired (Fig. 4, C–E). Finally, the death receptor Fas is found in characteristic clusters on the surface of Fas of Raf-1 KO cells, which are more sensitive to Fas-induced cell death (Fig. S3, A and B). All of these defects are caused by Rok- α hyperactivity and can be rescued by chemical inhibition of Rok- α , by expressing dominant-negative Rok- α , or by silencing the Rok- α gene (Ehrenreiter et al., 2005; Piazzolla et al., 2005).

Raf-1reg, but not the CRD mutant, also corrected all defects of Raf-1 KO cells: it significantly improved migration (Fig. 4 C), normalized cell shape, cortical actin bundles, and ezrin phosphorylation (Fig. 4, D and E). Finally, Raf-1reg reduced Fas surface clusters and cell death in Raf-1 KO cells (Fig. S3, A and B). These results demonstrate the biological relevance of the interaction between Rok- α and Raf-1reg and formally rule out a contribution of Raf-1 kinase activity to the regulation of cell shape, migration, and Fas expression.

Raf-1reg and Rok- α reg inhibit Rok- α -K in vivo

Our data suggest that the activity of the Rok- α kinase domain, restrained in cis by its own regulatory domain (Rok- α reg) before activation (Amano et al., 1999), is inhibited in trans by

Rok- α , FL Raf-1, constitutively active Ras (RasV12), or membrane-tethered SOS-F, resulting in the constitutive activation of endogenous Ras and the corresponding vectors (V). UT, untransfected COS-1 cells; *, endogenous Ras. Black lines indicate that intervening lanes have been spliced out. (E–G) Ras binding and subcellular localization affect Rok- α –Raf-1 interaction. (E) COS-1 cells were transfected with HA-tagged FL Rok- α and the indicated FL Raf-1 mutants. HA immunoprecipitates were analyzed and quantified as described in Fig. 1. (F) Fluorescence lifetime, GFP intensity, and mRFP1 intensity in MCF-7 cells transfected with GFP-FL Raf-1 WT or CC/SS mutant (donor) and mRFP1-Rok- α -K (acceptor). The cell marked with the asterisk was excluded from the cumulative FRET efficiency analysis in G as a result of insufficient photon counts (see Materials and methods). (G) Percentage of FRET efficiency is shown. (A, E, and G) Error bars indicate SD of three experiments. *, $P < 0.05$; **, $P < 0.01$; ***, $P < 0.005$. Bars: (B) 20 μ m; (F) 30 μ m.

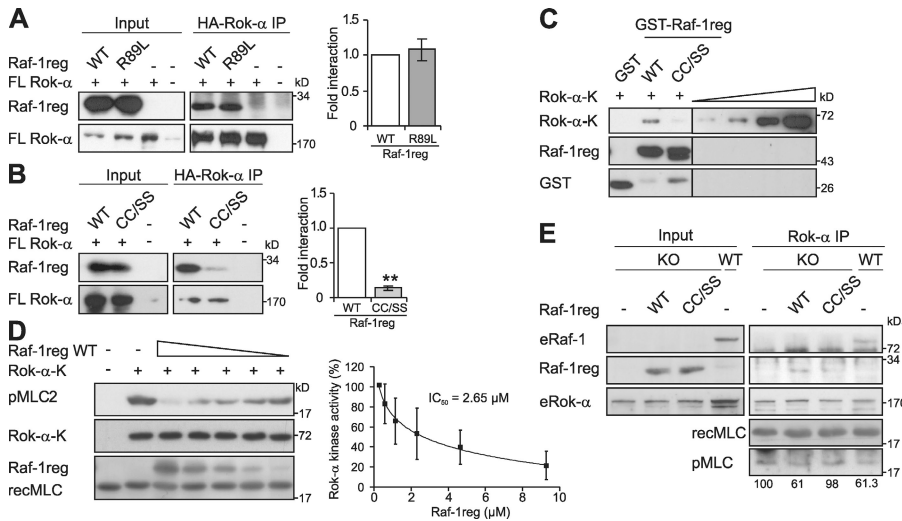


Figure 3. **Raf-1reg interacts with Rok-α and inhibits its kinase activity.** (A and B) CRD but not RBD mutation disrupts the binding of Raf-1reg to Rok-α. HA immunoprecipitates (IP) were analyzed as in Fig. 1. The mean \pm SD of at least three experiments is shown. **, $P < 0.01$. (C) Rok-α-K interacts in vitro with Raf-1reg WT but not with Raf-1reg CC/SS. 2 μ g GST, GST-Raf-1reg WT, or GST-Raf-1reg CC/SS on glutathione Sepharose beads were incubated with 25 ng His-tagged Rok-α-K. Rok-α-K and GST proteins were detected by immunoblotting with His and GST antibody. 3.125–25 ng recombinant Rok-α-K was loaded as a reference on the same gel. One representative experiment out of three is shown. Black lines indicate that intervening lanes have been spliced out. (D) Dose-dependent inhibition of Rok-α-K by purified Raf-1reg. 0.29–9.3 μ M Raf-1reg was incubated with 100 ng Rok-α-K (0.05 μ M) before a Rok kinase assay with 7 μ M recombinant MLC2 (recMLC2) as a substrate. The mean \pm SD of three experiments is

Raf-1reg once activation has occurred. A computational model of the Rok-α CRD, based on the structure of the autoinhibitory CRD of Raf-1 (Mott et al., 1996), is compatible with this idea (Fig. 5 A). More importantly, both Rok-αreg and Raf-1reg inhibit the activity of cotransfected Rok-α-K in vivo, reducing the phosphorylation of Rok-α downstream targets by a comparable

extent (Fig. 5 B). Finally, Rok-αreg and Raf-1reg, but not Raf-1reg CC/SS, reduced the hyperphosphorylation of ezrin as a result of hyperactive endogenous Rok-α in Raf-1 KO cells (Fig. 5 C). Thus, the regulatory domains of Rok-α and Raf-1 are similarly effective in regulating Rok-α activity in vivo, supporting a model in which activated Raf-1 modulates Rok-α

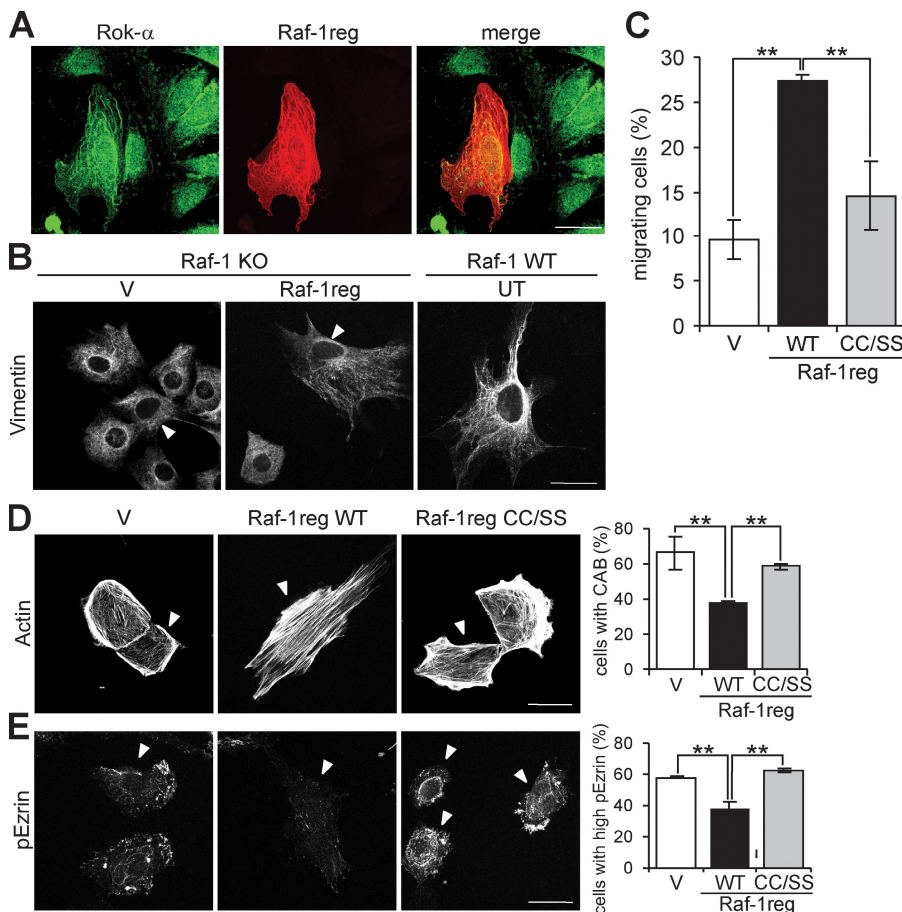


Figure 4. **Raf-1reg colocalizes with Rok-α and rescues all phenotypes of Raf-1 KO MEFs.** (A) Raf-1 KO MEFs expressing Raf-1reg were identified by staining with antibodies against Raf-1. The localization of Raf-1 and Rok-α in migrating MEFs was determined by immunofluorescence. (B–D) Raf-1reg improves cytoskeletal organization and migration. (B) Raf-1reg rescues vimentin cytoskeleton collapse in Raf-1 KO MEFs. Raf-1 KO MEFs cotransfected with pEGFP and pCMV (V) or pCMV Raf-1reg were stained with vimentin antibodies and analyzed by confocal microscopy. UT, untransfected cells. (C) Migration of Raf-1 KO MEFs transfected with the indicated pEGFP constructs was assessed using 10% FCS as a chemoattractant. The percentage of transfected cells migrating to the lower compartment of a Boyden chamber in 2.5 h is plotted. (D and E) Raf-1 KO MEFs were cotransfected with pEGFP and the indicated pCMV constructs, stained with phalloidin to visualize filamentous actin (D) or with anti-ezrin^{PT567} (E), and analyzed by confocal microscopy. The number of cells displaying cortical actin bundles (CAB) or prominent ezrin phosphorylation is plotted on the right. Arrowheads indicate EGFP-expressing cells. Error bars indicate SD of three experiments. **, $P < 0.01$. Bars, 20 μ m.

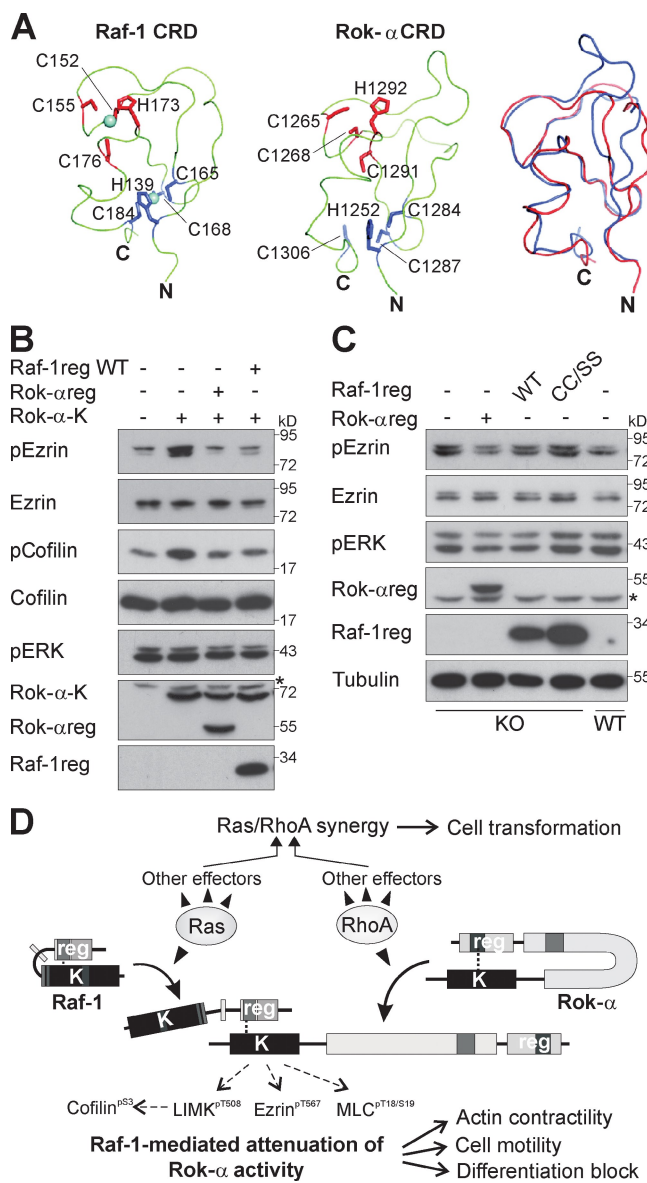


Figure 5. The regulatory domains of Raf-1 and Rok-α act as inhibitors of Rok-α kinase activity in vivo. (A) Comparison of the experimental solution structure of Raf-1 CRD (left) and the computational model of the Rok-α CRD (middle). Zinc cations are shown as spheres and the side chains of the residues coordinating the cations are shown as lines: red in one metal biosite and blue in the other. (right) Superposition of the Raf-1 and Rok-α CRDs. (B and C) COS-1 cells (B) and MEFs (C) were transfected with the indicated constructs. 24 h after transfection, cells were lysed and analyzed by immunoblotting. KO, Raf-1 KO MEFs; *, unspecific band. (D) Model of the regulation of Rok-α by Raf-1. GTPase binding disrupts intramolecular interaction between the regulatory and kinase domains of Raf-1 and Rok-α, upon which Raf-1 reg binds to the kinase domain of Rok-α, restraining Rho-induced Rok-α kinase activity. Inhibition in trans limits the phosphorylation of Rok-α downstream targets, regulating cell motility and differentiation.

by providing inhibition in trans (Fig. 5 D). Another GTPase-activated kinase, Pak1, is inhibited in trans in its basal state in the context of a homodimer in which the regulatory domain of one molecule inhibits the kinase domain of the other. However, although disruption of the dimer by activated GTPases allows Pak1 activation (Parrini et al., 2002), GTPase binding to both Raf-1 and Rok-α promotes the formation of complexes within which Rok-α activity is restrained by Raf-1.

Thus far, we don't have any evidence that Rok-α modulates Raf-1 activity. The Raf-1 kinase domain does not bind to Rok-α, and the regulatory domain is not a Rok-α substrate in vitro (unpublished data). It is possible that Rok-α regulates Raf-1 by promoting its localization to intermediate filaments, thereby bringing it in the proximity of specific substrates. Further studies will be needed to clarify this issue.

Implications for transformation

Ras, Rho, and their downstream effectors are implicated in tumorigenesis. A good example of Ras–Rho cross talk is the suppression of Rho signaling by Ras/ERK in transformed cells, leading to increased motility. This is achieved either at the level of integrin-mediated Rho activation, which is impaired by the product of the ERK target gene *fra-1* (Vial et al., 2003) or, more specifically, by uncoupling Rho activation from its downstream effector Rok. In particular, Rok expression can be reduced by ERK activation in Ras-transformed cells with high levels of active Rho (Sahai et al., 2001; Pawlak and Helfman, 2002b) and in v-src-transformed cells (Pawlak and Helfman, 2002a).

Our data identify a novel, ERK-independent mechanism by which Ras selectively regulates Rho signaling by promoting interaction between the top-tier kinases Raf-1 and Rok-α. We have recently shown the significance of this interaction in a model of Ras-driven epidermal tumorigenesis (Ehrenreiter et al., 2009) in which Ras causes transformation by inducing proliferation and survival (Sibilia et al., 2000) and by selectively blocking differentiation. We found that Ras mediates this block by promoting Raf-1–Rok-α interaction and the inhibition of Rok-α activity. If Raf-1 is ablated, both development and maintenance of the Ras-driven tumors are abrogated (Ehrenreiter et al., 2009). Understanding the mechanisms underlying the interaction between Raf-1 and Rok-α may hold promise for the design of novel, specific inhibitors for therapeutic treatments.

Materials and methods

Plasmids

The following plasmids were used in transient expression experiments: pXJ40-HA-FL Rok-α, ΔPH/CRD, Rok-α-K, Rok-αreg (Leung et al., 1996), pEFmyc FL Raf-1, pCMV5 FL Raf-1, Raf-1reg, Raf-1reg R89L (provided by W. Kolch, System Biology Institute, Dublin, Ireland; Kubicek et al., 2002; O'Neill et al., 2004), pEXV FL Raf-1, R89L, CC/SS, CAAX (provided by J.F. Hancock, University of Texas Medical School, Houston, TX; Roy et al., 1997), pEGFP Raf-1reg (provided by R.M. Lafrenie, Northern Ontario School of Medicine, Sudbury, Ontario, Canada; Zhang et al., 2002), pRSV FL Raf-1, Raf-1reg, and Raf-1-K (Bruder et al., 1992). For expression in bacteria, pGEX Raf-1reg (aa 1–187) was subcloned from pGEX Raf-1reg (aa 1–258; O'Neill et al., 2004) by PCR amplification and ligation. All CC/SS mutations were generated by site-directed mutagenesis and verified by sequencing. Monomeric RFP1 (mRFP1)–Rok-α constructs were generated by PCR amplification of pXJ40-HA–Rok-α and subcloned into the pcDNA mRFP1 vector. pGEX KG MLC2 and RhoA V14 Flag tagged were provided by E. Sahai (Cancer Research UK, London, England, UK) and A. Ridley (King's College London, London, England, UK), respectively.

Cell culture and transfection

3T3-like MEFs derived from *c-Raf-1*^{−/−} and WT embryos (Mikula et al., 2001), COS-1, MCF-7, and MDA-MB-468 cells (which express a high amount of EGF receptor; Filmus et al., 1985) were maintained in DME with 10% FCS and transiently transfected using Lipofectamine reagents (Invitrogen) according to the manufacturer's instructions.

Migration assay

Migration was assessed in a modified Boyden chamber as described previously (Ehrenreiter et al., 2005). Migrating and nonmigrating EGFP-transfected cells were visualized and quantified (≥ 450 cells/sample) by epifluorescence microscopy.

Immunofluorescence

Raf-1, Rok- α , vimentin, actin, ezrin pT567 , and Fas were performed as described previously (Ehrenreiter et al., 2005; Piazzolla et al., 2005). For Raf-1 and Rok- α staining, cells plated on fibronectin (Invitrogen) were permeabilized (0.01% Triton X-100), fixed in 4% PFA, and blocked with 0.2% gelatin before incubation with primary antibodies (Raf-1 and Rok- α ; BD) and staining with the appropriate Alexa Fluor 488- or 594-conjugated secondary antibodies (Invitrogen). Rhodamine-conjugated phalloidin (Invitrogen) was used to visualize actin filaments.

To visualize vimentin, intermediate filaments cells were fixed in methanol containing 5 mM EDTA and permeabilized with 0.5% Triton X-100. Cells were subsequently stained with vimentin antibody (Sigma-Aldrich) followed by Alexa Fluor 594-conjugated secondary antibodies.

For ezrin pT567 staining, cells were fixed in cold methanol/5 mM EDTA and blocked (10% goat serum/1% BSA) before incubation with phospho-ezrin-radixin-moesin antibody (pT567; Cell Signaling Technology) followed by Alexa Fluor 594-conjugated secondary antibodies.

For Fas staining, cells were fixed in cold methanol/5 mM EDTA for 10 min at room temperature followed by Alexa Fluor 594-conjugated secondary antibodies. Antifade reagent (ProLong Antifade; Invitrogen) was used as a mounting medium.

Confocal microscopy was performed at room temperature with a microscope (Axiovert 100M; Carl Zeiss, Inc.) fitted with a Plan Apochromat 63 \times /1.40 NA oil objective and equipped with the confocal laser-scanning module (LSM 510; Carl Zeiss, Inc.). Immersol (518; Carl Zeiss, Inc.) was used as imaging medium. Images were acquired using the LSM 510 software (version 2.3; Carl Zeiss, Inc.). Representative z stacks are shown. 600 transfected cells were counted for the quantification.

Cell lysates, immunoprecipitation, and immunoblotting

Cells were washed with ice-cold PBS and lysed in 200 mM Tris-HCl, pH 7.4, 2 mM EDTA, and 1% Triton X-100 with protease and phosphatase inhibitors. Lysates and HA-Rok- α immunoprecipitates were prepared from subconfluent cells 24–48 h after transfection and analyzed by immunoblotting using the following antibodies: Rok- α (Millipore), HA (12CA5), Rok- α , Raf-1, SOS (BD), pCofilin S3 , Cofilin, pMLC $^{T18/S19}$ (Santa Cruz Biotechnology, Inc.), pERK, pEzrin T567 , ezrin-radixin-moesin (Cell Signaling Technology), tubulin (Sigma-Aldrich), and pan-Ras V12 (EMD). The amount of Raf-1 proteins in the immunoprecipitation was quantified by densitometry (ImageQuant [GE Healthcare] or AlphaEase [Alpha Innotech]) and normalized to the amount of immunoprecipitated Rok- α .

Protein expression and purification

GST-Raf-1reg proteins were expressed in *Escherichia coli* Rosetta (DE3; EMD) by induction with 1 mM IPTG and incubation in minimal medium overnight at 22°C (Korz et al., 1995). GST-Raf-1reg proteins were purified by binding to glutathione Sepharose beads (GE Healthcare) and eluted with 20 mM reduced glutathione in 50 mM Tris-HCl, pH 8.0. Recombinant Raf-1reg and MLC2 were obtained by thrombin cleavage (6 U/ml overnight at 4°C) as previously described (Wyckoff et al., 2006).

GST pull-down and Rok- α in vitro kinase assays

GST-Raf-1reg immobilized on glutathione Sepharose was incubated with Rok- α -K (Millipore) for 15 min at 30°C, washed, and eluted by boiling in SDS sample buffer. Complex formation was determined by immunoblotting with anti-5His (QIAGEN) or anti-GST antibodies. Rok activity was assayed using 7 μ M MLC2 as a substrate. Phosphorylation was detected by immunoblotting with pMLC $^{T18/S19}$ antibody, normalized to MLC2 content, and quantified using an infrared imaging system (Odyssey; LI-COR Biosciences).

FRET determination by multiphoton FLIM

Time domain FLIM was performed at room temperature with a multiphoton microscope system comprised of a solid state-pumped (Verdi 8W; Coherent, Inc.), femtosecond self-mode-locked Ti:Sapphire laser system (Mira; Coherent, Inc.), an in-house-developed scan head, and an inverted microscope (TE2000E; Nikon; Peter et al., 2005; Festy et al., 2007). FRET was monitored by the conventional equation: FRET efficiency = $1 - \tau_{\text{do}}/\tau_{\text{control}}$, where τ_{do} is the lifetime of GFP-Raf-1 in cells that coexpress mRFP1-Rok- α ,

and τ_{control} is the GFP-Raf-1 lifetime measured in the absence of an acceptor. Because ≤ 100 -ps time resolution is achieved with our instrumentation, for a τ_{control} value of 2.35 ns, FRET efficiencies as low as 3% can be determined accurately. Pixel by pixel lifetime determination was achieved using a modified Levenberg–Marquardt fitting technique (Barber et al., 2005). The error in fitting the monoexponential decay model for fluorescence lifetime determination is $<0.4\%$ for signals with a peak of ≥ 500 photon counts. Also, in general, the lifetime of the interacting population (FRET species) can only be accurately determined with a peak photon count of ≥ 500 (Barber et al., 2009). We have therefore routinely excluded cells that have insufficient photon counts (<500 photons at the peak) from lifetime analysis.

Computational analysis of Raf-1 and Rok- α CRD

Rok- α CRD was modeled on the basis of the experimental structure of Raf-1 CRD (Protein Data Bank accession no. 1FAR; Mott et al., 1996) using Modeller (<http://saliweb.org/modeller/>; Marti-Renom et al., 2000) and refined with Jackal (full atom Amber force field; http://wiki.c2b2.columbia.edu/honiglab_public/index.php/Software:Jackal; Petrey et al., 2003) in the absence of the two zinc ions. The presence of two metal-binding sites was confirmed by two independent approaches, CheD (Babor et al., 2008) and MetSite (<http://bioinf.cs.ucl.ac.uk/MetSite/MetSite.html>; Sodhi et al., 2004).

Statistical analysis

All values are expressed as mean \pm SD of at least three independent experiments unless indicated otherwise. P-values were calculated using the unpaired, two-tailed Student's *t* test. $P \leq 0.05$ is considered statistically significant.

Online supplemental material

Fig. S1 shows that FL Raf-1 and Raf-1reg, but not the Raf-1 kinase domain, interact with FL Rok- α and Δ PH/CRD Rok- α . Fig. S2 shows that Raf-1reg, but not Raf-1reg CC/SS, inhibits the kinase activity of Rok- α in vitro. Fig. S3 shows that expression of Raf-1reg prevents the formation of Fas clusters at the cell surface of Raf-1 KO cells and reduces their sensitivity to Fas-induced cell death. Online supplemental material is available at <http://www.jcb.org/cgi/content/full/jcb.200906178/DC1>.

We thank M. Keppler (King's College London) for help constructing the plasmids used in the FLIM/FRET experiments.

This work was supported by the European Commission (grants LSH-CT-2006-037731 to M. Baccarini, I. Moarefi, and T. Ng and LSH-CT-2003-506803 to M. Baccarini), Fonds zur Förderung der wissenschaftlichen Forschung (grants P19530-B11 and VK-01 to M. Baccarini), and the Bioinformatics Integration Network III of the GEN-AU (to O. Carugo).

Submitted: 29 June 2009

Accepted: 6 October 2009

References

- Amano, M., K. Chihara, N. Nakamura, T. Kaneko, Y. Matsuura, and K. Kaibuchi. 1999. The COOH terminus of Rho-kinase negatively regulates rho-kinase activity. *J. Biol. Chem.* 274:32418–32424. doi:10.1074/jbc.274.45.32418
- Babor, M., S. Gerzon, B. Raveh, V. Sobolev, and M. Edelman. 2008. Prediction of transition metal-binding sites from apo protein structures. *Proteins*. 70:208–217. doi:10.1002/prot.21587
- Barber, P., S.M. Ameer-Beg, J. Gilbey, R.J. Edens, I. Ezike, and B. Vojnovic. 2005. Global and pixel kinetic data analysis for FRET detection by multi-photon time-domain FLIM. *Proc. SPIE*. 5700:171–181. doi:10.1117/12.590510
- Barber, P.R., S.M. Ameer-Beg, J. Gilbey, L.M. Carlin, M. Keppler, T.C. Ng, and B. Vojnovic. 2009. Multiphoton time-domain fluorescence lifetime imaging microscopy: practical application to protein–protein interactions using global analysis. *J. R. Soc. Interface*. 6:S93–S105. doi:10.1098/rsif.2008.0451.focus
- Bondeva, T., A. Balla, P. Várnai, and T. Balla. 2002. Structural determinants of Ras-Raf interaction analyzed in live cells. *Mol. Biol. Cell.* 13:2323–2333. doi:10.1091/mbc.E02-01-0019
- Bruder, J.T., G. Heidecker, and U.R. Rapp. 1992. Serum-, TPA-, and Ras-induced expression from Ap-1/ETs-driven promoters requires Raf-1 kinase. *Genes Dev.* 6:545–556. doi:10.1101/gad.6.4.545
- Catalanotti, F., G. Reyes, V. Jesenberger, G. Galabova-Kovacs, R. de Matos Simoes, O. Carugo, and M. Baccarini. 2009. A Mek1-Mek2 heterodimer determines the strength and duration of the Erk signal. *Nat. Struct. Mol. Biol.* 16:294–303. doi:10.1038/nsmb.1564

Chen, X.Q., I. Tan, C.H. Ng, C. Hall, L. Lim, and T. Leung. 2002. Characterization of RhoA-binding kinase ROKalpha implication of the pleckstrin homology domain in ROKalpha function using region-specific antibodies. *J. Biol. Chem.* 277:12680–12688. doi:10.1074/jbc.M109839200

Cutler, R.E. Jr., R.M. Stephens, M.R. Saracino, and D.K. Morrison. 1998. Autoregulation of the Raf-1 serine/threonine kinase. *Proc. Natl. Acad. Sci. USA* 95:9214–9219. doi:10.1073/pnas.95.16.9214

Dvorsky, R., L. Blumenstein, I.R. Vetter, and M.R. Ahmadian. 2004. Structural insights into the interaction of ROCKI with the switch regions of RhoA. *J. Biol. Chem.* 279:7098–7104. doi:10.1074/jbc.M311911200

Eblen, S.T., J.K. Slack-Davis, A. Tarcsafalvi, J.T. Parsons, M.J. Weber, and A.D. Catling. 2004. Mitogen-activated protein kinase feed-back phosphorylation regulates MEK1 complex formation and activation during cellular adhesion. *Mol. Cell. Biol.* 24:2308–2317. doi:10.1128/MCB.24.6.2308-2317.2004

Ehrenreiter, K., D. Piazzolla, V. Velamoor, I. Sobczak, J.V. Small, J. Takeda, T. Leung, and M. Baccarini. 2005. Raf-1 regulates Rho signaling and cell migration. *J. Cell Biol.* 168:955–964. doi:10.1083/jcb.200409162

Ehrenreiter, K., F. Kern, V. Velamoor, K. Meissl, G. Galabova-Kovacs, M. Sibilia, and M. Baccarini. 2009. Raf-1 addiction in Ras-induced skin carcinogenesis. *Cancer Cell.* 16:149–160. doi:10.1016/j.ccr.2009.06.008

Festy, F., S.M. Ameer-Beg, T. Ng, and K. Suhling. 2007. Imaging proteins in vivo using fluorescence lifetime microscopy. *Mol. Biosyst.* 3:381–391. doi:10.1039/b617204k

Filmus, J., M.N. Pollak, R. Cailleau, and R.N. Buick. 1985. MDA-468, a human breast cancer cell line with a high number of epidermal growth factor (EGF) receptors, has an amplified EGF receptor gene and is growth inhibited by EGF. *Biochem. Biophys. Res. Commun.* 128:898–905. doi:10.1016/0006-291X(85)90131-7

Heasman, S.J., and A.J. Ridley. 2008. Mammalian Rho GTPases: new insights into their functions from in vivo studies. *Nat. Rev. Mol. Cell Biol.* 9:690–701. doi:10.1038/nrm2476

Korz, D.J., U. Rinas, K. Hellmuth, E.A. Sanders, and W.D. Deckwer. 1995. Simple fed-batch technique for high cell density cultivation of *Escherichia coli*. *J. Biotechnol.* 39:59–65. doi:10.1016/0168-1656(94)00143-Z

Kubicek, M., M. Pacher, D. Abraham, K. Podar, M. Eulitz, and M. Baccarini. 2002. Dephosphorylation of Ser-259 regulates Raf-1 membrane association. *J. Biol. Chem.* 277:7913–7919. doi:10.1074/jbc.M108733200

Leevers, S.J., H.F. Paterson, and C.J. Marshall. 1994. Requirement for Ras in Raf activation is overcome by targeting Raf to the plasma membrane. *Nature*. 369:411–414. doi:10.1038/369411a0

Leung, T., X.Q. Chen, E. Manser, and L. Lim. 1996. The p160 RhoA-binding kinase ROK alpha is a member of a kinase family and is involved in the reorganization of the cytoskeleton. *Mol. Cell. Biol.* 16:5313–5327.

Martí-Renom, M.A., A.C. Stuart, A. Fiser, R. Sánchez, F. Melo, and A. Sali. 2000. Comparative protein structure modeling of genes and genomes. *Annu. Rev. Biophys. Biomol. Struct.* 29:291–325. doi:10.1146/annurev.biophys.29.1.291

Mikula, M., M. Schreiber, Z. Husak, L. Kucerova, J. Rüth, R. Wieser, K. Zatloukal, H. Beug, E.F. Wagner, and M. Baccarini. 2001. Embryonic lethality and fetal liver apoptosis in mice lacking the c-raf-1 gene. *EMBO J.* 20:1952–1962. doi:10.1093/emboj/20.8.1952

Mott, H.R., J.W. Carpenter, S. Zhong, S. Ghosh, R.M. Bell, and S.L. Campbell. 1996. The solution structure of the Raf-1 cysteine-rich domain: a novel ras and phospholipid binding site. *Proc. Natl. Acad. Sci. USA* 93:8312–8317. doi:10.1073/pnas.93.16.8312

O'Neill, E., L. Rushworth, M. Baccarini, and W. Kolch. 2004. Role of the kinase MST2 in suppression of apoptosis by the proto-oncogene product Raf-1. *Science*. 306:2267–2270. doi:10.1126/science.1103233

Olson, M.F. 2008. Applications for ROCK kinase inhibition. *Curr. Opin. Cell Biol.* 20:242–248. doi:10.1016/j.cub.2008.01.002

Parrini, M.C., M. Lei, S.C. Harrison, and B.J. Mayer. 2002. Pak1 kinase homodimers are autoinhibited in trans and dissociated upon activation by Cdc42 and Rac1. *Mol. Cell.* 9:73–83. doi:10.1016/S1097-2765(01)00428-2

Pawlak, G., and D.M. Helfman. 2002a. MEK mediates v-Src-induced disruption of the actin cytoskeleton via inactivation of the Rho-ROCK-LIM kinase pathway. *J. Biol. Chem.* 277:26927–26933. doi:10.1074/jbc.M202261200

Pawlak, G., and D.M. Helfman. 2002b. Post-transcriptional down-regulation of ROCKI/Rho-kinase through an MEK-dependent pathway leads to cytoskeleton disruption in Ras-transformed fibroblasts. *Mol. Biol. Cell.* 13:336–347. doi:10.1091/mbc.01-06-0302

Peter, M., S.M. Ameer-Beg, M.K. Hughes, M.D. Keppler, S. Prag, M. Marsh, B. Vejnovic, and T. Ng. 2005. Multiphoton-FLIM quantification of the EGFP-mRFP1 FRET pair for localization of membrane receptor-kinase interactions. *Biophys. J.* 88:1224–1237. doi:10.1529/biophysj.104.050153

Petrey, D., Z. Xiang, C.L. Tang, L. Xie, M. Gimpelev, T. Mitros, C.S. Soto, S. Goldsmith-Fischman, A. Kurnytsky, A. Schlessinger, et al. 2003. Using multiple structure alignments, fast model building, and energetic analysis in fold recognition and homology modeling. *Proteins*. 53(Suppl 6):430–435. doi:10.1002/prot.10550

Piazzolla, D., K. Meissl, L. Kucerova, C. Rubiolo, and M. Baccarini. 2005. Raf-1 sets the threshold of Fas sensitivity by modulating Rok- α signaling. *J. Cell Biol.* 171:1013–1022. doi:10.1083/jcb.200504137

Riento, K., and A.J. Ridley. 2003. Rocks: multifunctional kinases in cell behaviour. *Nat. Rev. Mol. Cell Biol.* 4:446–456. doi:10.1038/nrm1128

Roy, S., A. Lane, J. Yan, R. McPherson, and J.F. Hancock. 1997. Activity of plasma membrane-recruited Raf-1 is regulated by Ras via the Raf zinc finger. *J. Biol. Chem.* 272:20139–20145. doi:10.1074/jbc.272.32.20139

Sahai, E., M.F. Olson, and C.J. Marshall. 2001. Cross-talk between Ras and Rho signalling pathways in transformation favours proliferation and increased motility. *EMBO J.* 20:755–766. doi:10.1093/emboj/20.4.755

Shimizu, T., K. Ihara, R. Maesaki, M. Amano, K. Kaibuchi, and T. Hakoshima. 2003. Parallel coiled-coil association of the RhoA-binding domain in Rho-kinase. *J. Biol. Chem.* 278:46046–46051. doi:10.1074/jbc.M306458200

Sibilia, M., A. Fleischmann, A. Behrens, L. Stingl, J. Carroll, F.M. Watt, J. Schlessinger, and E.F. Wagner. 2000. The EGF receptor provides an essential survival signal for SOS-dependent skin tumor development. *Cell*. 102:211–220. doi:10.1016/S0092-8674(00)00026-X

Sin, W.C., X.Q. Chen, T. Leung, and L. Lim. 1998. RhoA-binding kinase alpha translocation is facilitated by the collapse of the vimentin intermediate filament network. *Mol. Cell. Biol.* 18:6325–6339.

Sodhi, J.S., K. Bryson, L.J. McGuffin, J.J. Ward, L. Wernisch, and D.T. Jones. 2004. Predicting metal-binding site residues in low-resolution structural models. *J. Mol. Biol.* 342:307–320. doi:10.1016/j.jmb.2004.07.019

Terai, K., and M. Matsuda. 2005. Ras binding opens c-Raf to expose the docking site for mitogen-activated protein kinase kinase. *EMBO Rep.* 6:251–255. doi:10.1038/sj.embor.7400349

Tian, T., A. Harding, K. Inder, S. Plowman, R.G. Parton, and J.F. Hancock. 2007. Plasma membrane nanoswitches generate high-fidelity Ras signal transduction. *Nat. Cell Biol.* 9:905–914. doi:10.1038/ncb1615

Vial, E., E. Sahai, and C.J. Marshall. 2003. ERK-MAPK signaling coordinately regulates activity of Rac1 and RhoA for tumor cell motility. *Cancer Cell*. 4:67–79. doi:10.1016/S1535-6108(03)00162-4

Wellbrock, C., M. Karasarides, and R. Marais. 2004. The RAF proteins take centre stage. *Nat. Rev. Mol. Cell Biol.* 5:875–885. doi:10.1038/nrm1498

Williams, J.G., J.K. Drugan, G.S. Yi, G.J. Clark, C.J. Der, and S.L. Campbell. 2000. Elucidation of binding determinants and functional consequences of Ras/Raf-cysteine-rich domain interactions. *J. Biol. Chem.* 275:22172–22179. doi:10.1074/jbc.M000397200

Wyckoff, J.B., S.E. Pinner, S. Gschmeissner, J.S. Condeelis, and E. Sahai. 2006. ROCK- and myosin-dependent matrix deformation enables protease-independent tumor-cell invasion in vivo. *Curr. Biol.* 16:1515–1523. doi:10.1016/j.cub.2006.05.065

Yamaguchi, O., T. Watanabe, K. Nishida, K. Kashiwase, Y. Higuchi, T. Takeda, S. Hikoso, S. Hirotani, M. Asahi, M. Taniike, et al. 2004. Cardiac-specific disruption of the c-raf-1 gene induces cardiac dysfunction and apoptosis. *J. Clin. Invest.* 114:937–943.

Zhang, L., M. Bewick, and R.M. Lafrenie. 2002. Role of Raf-1 and FAK in cell density-dependent regulation of integrin-dependent activation of MAP kinase. *Carcinogenesis*. 23:1251–1258. doi:10.1093/carcin/23.7.1251

Zhao, Z.S., and E. Manser. 2005. PAK and other Rho-associated kinases—effectors with surprisingly diverse mechanisms of regulation. *Biochem. J.* 386:201–214. doi:10.1042/BJ20041638